Journal of Basic and Applied Research International
6(4): 239-247, 2015
International Knowledge Press
www.ikpress.org

THERMOELECTRIC PROPERTIES OF A SERIALLY COUPLED T-SHAPE-DOUBLE-QUANTUM DOT STRUCTURE

L. F. AL-BADRY[1*], J. M. AL-MUKH[2] AND S. I. EASA[3]
[1]Department of Physics, College of Science, University of Thi-Qar, Thi-Qar, Iraq.
[2]Department of Physics, College of Education for Pure Science, University of Basrah, Basrah, Iraq.

AUTHORS' CONTRIBUTIONS
This work was carried out in collaboration between all authors. Author LFAB designed the study, wrote the protocol and interpreted the data. Author SIE anchored the field study, gathered the initial data and performed preliminary data analysis. While authors JMAM managed the literature searches and produced the initial draft. All authors read and approved the final manuscript.

Received: 24th February 2015
Accepted: 11th March 2015
Published: 7th April 2015

Original Research Article

ABSTRACT

In this paper, we present our theoretical treatment for electron transport through aserially coupled T-shape-double-quantum dotstructure attached to the donor and left lead on the left side, while on the right side it is attached to the acceptor and right lead. Our treatment is based on the time-dependent Anderson-Newns Hamiltonian neglecting the correlation effects. The equations of motion are derived for all subsystems, then the steady state is considered to obtain an analytical expression for the transmission probability as a function of the system energies. The subsystems eigenvalues, the coupling interaction between them as well as the leads band width all are taken into consideration and highlighted. We employ the transmission probability to calculate the thermoelectric properties for this structure and investigate quantum interference effects on the thermoelectric properties.

Keywords: Quantum dot; thermoelectric properties; figure of merit; antiresonance.

1. INTRODUCTION

Energy conversion based on thermoelectric properties of solid-state materials has been attracting recently renewed attention, especially in the case of nanostructures [1,2]. Theoretical predictions [3-5] as well as experiments [6-8] show that nanostructures exhibit higher efficiencies than bulk materials,making them very attractive for their potential application in energy-conversion and cooling devices. The thermoelectric efficiency of thermoelectric devices measured by a dimensionless figure of merit *ZT*. A figure of meritused to characterize the performance of a device. Figure of merit can be calculated by the following formula $ZT = S^2GT/(\kappa_{el} + \kappa_{ph})$, where S is the thermopower, G is electrical conductance, T is the temperature in metallic electrodes, κ_{el} and κ_{ph} are electron and phonon thermal conductance, respectively [9].

To increase the magnitude of dimensionless figure of merit *ZT*, large thermopower, high electrical conductance, and low thermal conductance are required. However, these physical quantities

**Corresponding author: Email: albadrylafy@yahoo.com;*

areinterdependent in bulk materials according to the Wiedemann-Franz law that the quantity κ/GT remains constant [3]. Therefore thermoelectric efficiency in bulk materials rarely exceed 1 [10]. To enhance the thermoelectric efficiency, many approaches have been proposed, and one of which is to reduce the system dimensionality.

Some higher values of S and ZT were found in low-dimensional systems due to its sharp change in the density of states near the Fermi level [11,12] and the significant reduction of phonon thermal conductance κ_{ph} due to the strong phonon scattering by the interfaces between the nanostructures [13].

However, due to the quantum nature of the electrons, the thermoelectric properties are determined by quantum effects [14,15]. The small sizes of QDs make the phase coherent of waves become more important, and quantum interference phenomena originate when the particles moves along different transport paths [16].

It is well known that, the zero point of the conductance spectrum, called antiresonance, originates from the destructive quantum interference among electron waves passing through different transmission paths [17]. With respect to the coupled-QD structures, the typical ones are the structures of the so-called T-shaped QDs [18-22]. A unique property of electron transport through the T-shaped QD systems is that the positions of the antiresonance coincide with the eigenvalues of the side-coupled QDs [17].

In this work, we will present our theoretical treatment to formulate expression for the transmission probability of the electron transport throughout a serially coupled T-shape-double-quantum dot structure to study and calculate the thermoelectric properties for the considered system. So, all the system eigenvalues and coupling interactions are taken into consideration to give obvious view for the system dynamics.

2. THEORY

In this work, the considered system is left lead-donor-serially coupled T-shape-double-quantum dot-acceptor-right lead see Fig. 1, where the chain consists of N quantum dotsconnection like T-shape. General formula for the transmission probability of this systemwill be derived, which is described by using time-dependent and spin less Anderson-Newns Hamiltonian [23] neglecting thecorrelationinteractions in all subsystems.Anderson-Newns Hamiltonianis a very rich Hamiltonian, which is capable of describing a diversity of physical situations, depending on the values of correlation interactions and coupling interaction between subsystems, and of the degeneracy of the local states.

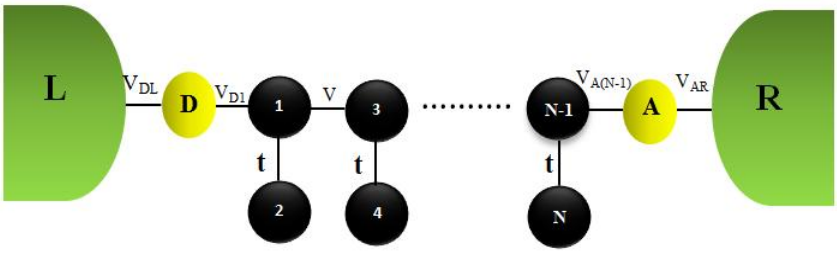

Fig. 1. Shows serially coupled T-shape-double-quantum dot structure

The Hamiltonian of system is given by:

$$H(t) = E_D n_D(t) + E_A n_A(t) + \sum_{n=1}^{N} E_n n_n(t) + \sum_{k_L} E_{k_L} n_{k_L}(t) + \sum_{k_R} E_{k_R} n_{k_R}(t) + \left(V_{D1} C_D^{\dagger}(t) C_1(t) + H.C.\right)$$
$$+\left(V_{A(N-1)} C_A^{\dagger}(t) C_{N-1}(t) + H.C.\right) + \sum_{n=odd}^{N-3} \left(V_{n(n+2)} C_n^{\dagger}(t) C_{n+2}(t) + H.C.\right)$$
$$+ \sum_{n=odd}^{N-1} \left(t_{n(n+1)} C_n^{\dagger}(t) C_{n+1}(t) + H.C.\right) + \sum_{k_L} \left(V_{Dk_L} C_D^{\dagger}(t) C_{k_L}(t) + H.C.\right)$$
$$+ \sum_{k_R} \left(V_{Ak_R} C_A^{\dagger}(t) C_{k_R}(t) + H.C.\right) \quad (1)$$

where $n_j(t) = C_j^{\dagger}(t)C_j(t)$ and $C_j^{\dagger}(t)(C_j(t))$ denotes annihilation (creation) operators, with $j = D, A, n, k_L$ and k_R. The index k_i being a set of quantum numbers, with $i = L, R$. Notably, the summation in the third term in Eq. (1) is over all quantum dots (each one with one effective energy level E_n). The sixthterm is concerning the coupling interaction between the donor(with one effective energy level E_D) with quantum dot of number 1. The seventh term is concerning the coupling interaction between the acceptor (with one effective energy level E_A) with quantum dot of number $(N-1)$. The eighth term describes the interdot interactions between central quantum dot. While the ninth term represents the interdot interactions between central quantum dot and side quantum dot.In this formula, we consider the number 1 is the one that connected to the donor while the quantum dot number (N-1) is the one that connected to the acceptor.

The equations of motion for $C_j(t)$ can be obtained by using [24],

$$\dot{C}_j(t) = -i\frac{dH(t)}{dC_j^{\dagger}(t)} \tag{2}$$

to get,

$$\dot{C}_D(t) = -iE_D C_D(t) - iV_{D1}C_1(t) - i\sum_{k_L} V_{Dk_L}C_{k_L}(t) \tag{3}$$

$$\dot{C}_A(t) = -iE_A C_A(t) - iV_{A(N-1)}C_{N-1}(t) - i\sum_{k_R} V_{Ak_R}C_{k_R}(t) \tag{4}$$

$$\dot{C}_1(t) = -iE_1 C_1(t) - iV_{1D}C_D(t) - iV_{13}C_3(t) - it_{12}C_2(t) \tag{5}$$

$$\dot{C}_{n+1}(t) = -iE_{n+1}C_{n+1}(t) - it_{(n+1)n}C_n(t) for: odd \tag{6}$$

$$\dot{C}_{n+2}(t) = -iE_{n+2}C_{n+2}(t) - iV_{(n+2)n}C_n(t) - iV_{(n+2)(n+4)}C_{n+4}(t) - it_{(n+2)(n+3)}C_{n+3}(t) \quad for: odd \tag{7}$$

$$\dot{C}_{N-1}(t) = -iE_{N-1}C_{N-1}(t) - iV_{(N-1)A}C_A(t) - it_{(N-1)N}C_N(t) - iV_{(N-1)N-3}C_{N-3}(t) \tag{8}$$

$$\dot{C}_{k_L}(t) = -iE_{k_L}C_{k_L}(t) - iV_{k_L D}C_D(t) \tag{9}$$

$$\dot{C}_{k_R}(t) = -iE_{k_R}C_{k_R}(t) - iV_{k_R A}C_A(t) \tag{10}$$

Where $\dot{C}_{n+1}(t)$ for even numbered dots, while $\dot{C}_{n+2}(t)$ for odd numbered dots

For steady state, we define $C_j(t)$ by the following:

$$C_j(t) = \bar{C}_j(E)e^{-iEt} \tag{11}$$

where *E* denotes the system eigenvalues, then accordingly,$\dot{\bar{C}}_j(E) = 0$

$$\bar{C}_D(E)(E - E_D) = V_{D1}\bar{C}_1(E) + \sum_{k_L} V_{Dk_L}\bar{C}_{k_L}(E) \tag{12}$$

$$\bar{C}_A(E)(E - E_A) = V_{A(N-1)}\bar{C}_{N-1}(E) + \sum_{k_R} V_{Ak_R}\bar{C}_{k_R}(E) \tag{13}$$

$$\bar{C}_1(E)(E - E_1) = V_{1D}\bar{C}_D(E) + V_{13}\bar{C}_3(E) + t_{12}\bar{C}_2(E) \tag{14}$$

$$\bar{C}_{n+1}(E)(E-E_{n+1}) = t_{(n+1)n}\bar{C}_n(E) \tag{15}$$

$$\bar{C}_{n+2}(E)(E-E_{n+2}) = V_{(n+2)n}\bar{C}_n(E) + V_{(n+2)(n+4)}\bar{C}_{n+4}(E) + t_{(n+2)(n+3)}\bar{C}_{n+3}(E) \tag{16}$$

$$\bar{C}_{N-1}(E)(E-E_{N-1}) = V_{(N-1)A}\bar{C}_A(E) + t_{(N-1)N}\bar{C}_N(E) + V_{(N-1)N-3}\bar{C}_{N-3}(E) \tag{17}$$

$$\bar{C}_{k_L}(E)\left(E-E_{k_L}\right) = V_{k_LD}\bar{C}_D(E) \tag{18}$$

$$\bar{C}_{k_R}(E)\left(E-E_{k_R}\right) = V_{k_RA}\bar{C}_A(E) \tag{19}$$

Then the transmission probability amplitude and the transmission probability can be calculated respectively as,

$$t(E) = \frac{\bar{C}_A(E)}{\bar{C}_D(E)} \tag{20}$$

$$T(E) = |t(E)|^2 \tag{21}$$

Now, by substituting Eq. (19) in Eq. (13) we obtain,

$$\bar{C}_A(E)\left(E - E_A - \sum\nolimits_{AR}(E)\right) = V_{A(N-1)}\bar{C}_{N-1}(E) \tag{22}$$

where $\sum_{AR}(E) = \sum_{k_R}\frac{\left|V_{Ak_R}\right|^2}{E-E_{k_R}}$ is the level self-energy [22]

We rearranged the set of linear Eqs. (14-17) in a matrix-form equation,

$$\begin{vmatrix} E-E_1 & -t_{12} & -V_{13} & 0 & 0 \\ -t_{21} & E-E_2 & 0 & 0 & 0 \\ -V_{31} & 0 & \ddots & \ddots & \vdots \\ 0 & 0 & \ddots & E-E_{N-1} & -t_{(N-1)N} \\ 0 & 0 & 0 & -t_{N(N-1)} & E-E_N \end{vmatrix} \begin{vmatrix} \bar{C}_1 \\ \bar{C}_2 \\ \vdots \\ \bar{C}_{N-1} \\ \bar{C}_N \end{vmatrix} = \begin{vmatrix} V_{1D}\bar{C}_D \\ 0 \\ \vdots \\ V_{(N-1)A}\bar{C}_A \\ 0 \end{vmatrix} \tag{23}$$

Accordingly, the transmission probability amplitude is,

$$t(E) = \frac{\bar{C}_A}{\bar{C}_D} = \frac{V_{A(N-1)}\Delta_{1D}/\Delta}{\left(E - E_A - V_{A(N-1)}\Delta_{(N-1)A}/\Delta\right) - \sum_{AR}(E)} \tag{24}$$

Then the transmission probability is $T(E) = |t(E)|^2$, which will employed for calculation the thermoelectric properties. Where the determinant Δ is defined as,

$$\Delta = \begin{vmatrix} E-E_1 & -t_{12} & -V_{13} & 0 & 0 \\ -t_{21} & E-E_2 & 0 & 0 & 0 \\ -V_{31} & 0 & \ddots & \ddots & \vdots \\ 0 & 0 & \ddots & E-E_{N-1} & -t_{(N-1)N} \\ 0 & 0 & 0 & -t_{N(N-1)} & E-E_N \end{vmatrix} \tag{25}$$

And one can obtain the determinant $\Delta_{(N-1)A}$ by substituting the right side of Eq. (23) in the (N-1) the column of Eq. (25), making $V_{1D}\bar{C}_D = 0$, while one can also obtain the determinant Δ_{1D} by substituting the right side of Eq. (23) in the first column of Eq. (25), making $V_{(N-1)A}\bar{C}_A = 0$.

The thermoelectric properties of the system calculated as follows: If one assumes an effective drop voltage ΔV and a temperature difference ΔT between the left and right leads. Then, in the linear temperature and bias regime, the charge current I_e and the heat current I_Q through the system are given by [25]:

$$I_e = \frac{2}{h}\left(e^2 K_0 \Delta V - \frac{e}{T} K_1 \Delta T\right) \quad (26)$$

$$I_Q = \frac{2}{h}\left(-eK_1 \Delta V + \frac{1}{T} K_2 \Delta T\right) \quad (27)$$

with h is Planck constant. The transport coefficients are computed by using the integrals [25],

$$K_n(\mu, T) = \int (-\frac{\partial f}{\partial E})(E-\mu)^n T(E) dE \quad (28)$$

μ is the chemical potential and $f_\beta(E)$ is the Fermi distribution function, with $f_\beta(E) = 1/(1 + exp\frac{(E-\mu_\beta)}{k_B T})$ for the lead β $(= L, R)$ and k_B being the Boltzmann constant, where $\mu_L = \mu_R = \mu$.

The most suitable parameter todescribe the electron transport throughout nanostructured systemis the electrical conductance $G = -I_e/\Delta V$, it can be obtained by using Eq. (26), which is calculated at zero temperature gradient,

$$G = \frac{2e^2}{h} K_0 \quad (29)$$

where $2e^2/h$ is conductance quantum. The thermopower S is defined as the voltage drop induced by the difference of temperature when the charge current I_e (Eq.26) vanishes, and it is given by:

$$S = -\frac{\Delta V}{\Delta T} = -\frac{1}{eT}\frac{K_1}{K_0}. \quad (30)$$

And the electron thermal conductance $\kappa_{el} = -I_Q/\Delta T$ can be obtained by Eq. (27), when the charge current I_e vanishes,

$$\kappa_{el} = \frac{2}{hT}\left(K_2 - \frac{K_1^2}{K_0}\right) \quad (31)$$

Finally one can obtain figure of merit by using the following formula,

$$ZT = \frac{1}{\frac{K_0 K_2}{K_1^2} - 1} \quad (32)$$

where we have neglected the phonon thermal conductance.

3. CALCULATIONS AND DISCUSSION

For semi-infinite atomic chain for the leads, the density of electronic states for right lead is given by [26],

$$\rho_R(E) = \frac{1}{\pi|\beta_R|}\sqrt{1 - \left(\frac{E - E_{FR}}{2\beta_R}\right)^2} \quad (33)$$

where E_{FR} is the position of Fermi energy level at the right lead. β_R is related to the energy band width$\equiv 4\beta_R$ of the right lead. The self-energy $\sum_{AR}(E)$ is written as [22],

$$\sum\nolimits_{AR}(E) = -i\Delta_{AR}(E) + \Lambda_{AR}(E) \quad (34)$$

with $\Delta_{AR}(E)$ is the acceptor level broadening due to acceptor level-right lead's levels coupling interaction. $\Lambda_{AR}(E)$ is the quantum shift that happens in the acceptor level due to the over mentioned coupling interactions. With [27],

$$\Delta_{AR}(E) = \pi|V_{AR}|^2 \rho_R(E) \quad (35)$$

and,

$$\Lambda_{AR}(E) = P\frac{1}{\pi}\int \frac{\Delta_{AR}(E')}{E - E'} dE' \quad (36)$$

where P refers to the principal part.

For all our results that presented in Figs. 2-5, the energies are given by Γ, the energy levels of the sites are chosen as E_n=0 and the coupling interaction between subsystems are $V = \Gamma$, $V_{1D} = V_{(N-1)A} = \Gamma$, and $V_{AR} = 1.3\Gamma$. While the interdot interaction between the central quantum dots and side quantum dots$t = 0.2\Gamma, 0.6\Gamma,$ and Γ.

We calculate the thermoelectric properties assisted with antiresonance of a serially coupled T-shape-double- quantum dot. Fig. 2 shows electrical conductance of this structure, which calculated by Eq. (29), where anantiresonance appears at the energy level of side quantum dot. This feature appears due to the quantum interference effect between a localized state on the side quantum dot with the continuum of the central quantum dot coupled to the donor and the acceptor. Antiresonance increases when interdot interaction between the central quantum dot and side quantum dot (t) increases, it becomesalso wider.

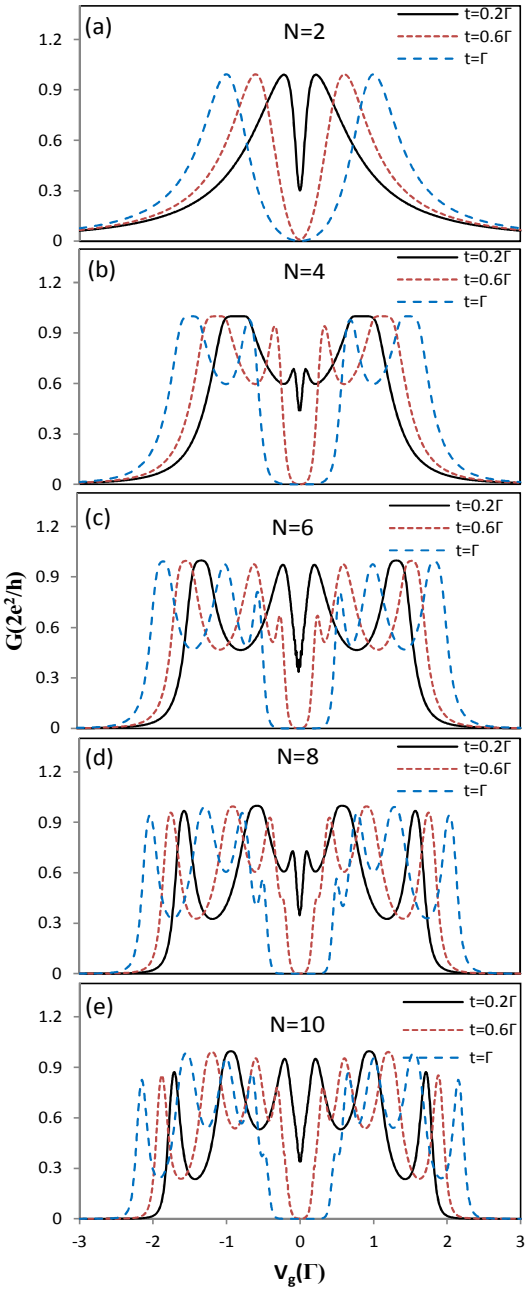

Fig. 2. Electrical conductance as a function of gate voltage $V_g$for (a) two quantum dots, (b) four quantum dots, (c) six quantum dots, (d) eight quantum dots, and (e) ten quantum dots, with E_n=0, V=V_{DB}=V_{AB}=Γ, t=0.2, 0.6 and Γ, V_{AR}=1.3Γ, T=300K

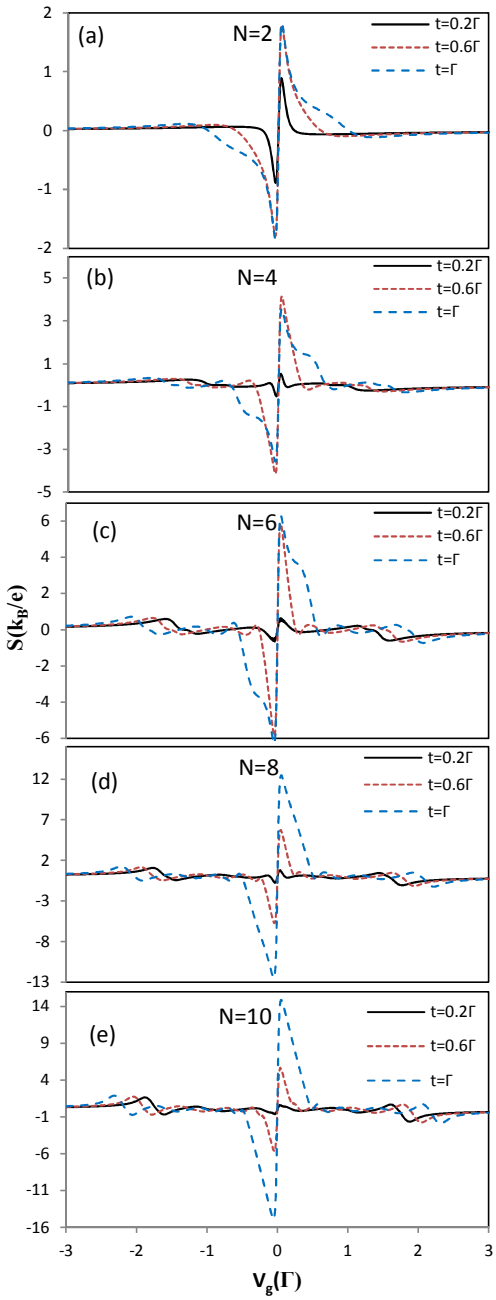

Fig. 3. The thermopower as a function of gate voltage $V_g$for (a) two quantum dots, (b) four quantum dots, (c) six quantum dots, (d) eight quantum dots, and (e) ten quantum dots, with E_n=0, V=V_{DB}=V_{AB}=Γ, t=0.2, 0.6 and Γ, V_{AR}=1.3Γ, T=300K

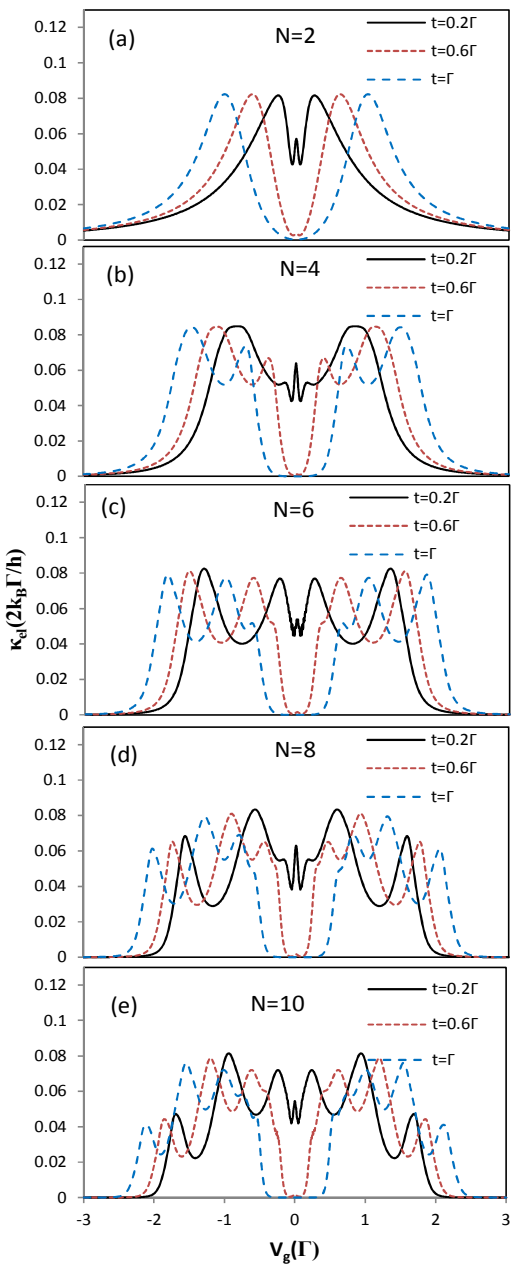

Fig. 4. Electron thermal conductance as a function of gate voltage $V_g$for (a) two quantum dots, (b) four quantum dots, (c) six quantum dots, (d) eight quantum dots, and (e) ten quantum dots, with E_n=0, V=V_{DB}=V_{AB}=Γ, t=0.2, 0.6 and Γ, V_{AR}=1.3Γ,T=300K

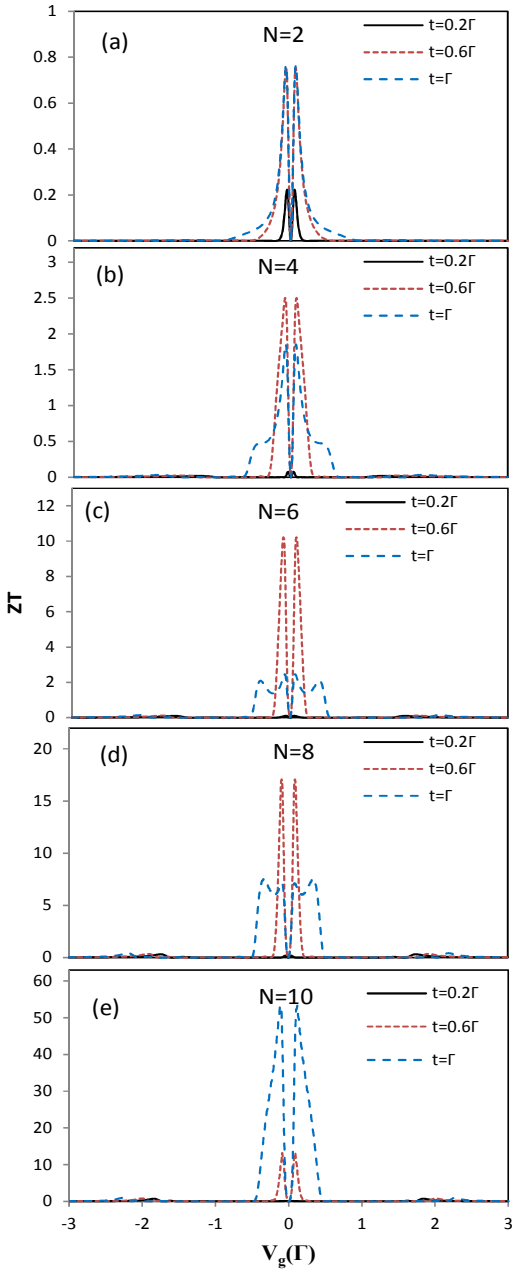

Fig. 5. Figure of merit as a function of gate voltage $V_g$for (a) two quantum dots, (b) four quantum dots, (c) six quantum dots, (d) eight quantum dots, and (e) ten quantum dots, with E_n=0, V=V_{DB}=V_{AB}=Γ, t=0.2, 0.6 and Γ, V_{AR}=1.3Γ,T=300K

In Figs. 2(a) and 2(b), the number of resonances equal to the number of quantum dots for all values of t.Also this characteristic appears in Figs. 2(c) and 2(d) at $t = 0.6\Gamma, \Gamma$, while the number of resonances reduced to $(N-2)$ at $t = 0.2\Gamma$. When $N = 10$ the number of resonances decreased to $N-4$ at $t = 0.2\Gamma$, as shown in Fig. 2(e). The number of resonances relative to the number of quantum dots clearly suppressed by increasing N and decreasing t. The number of quantum dots insignificantly effect on the magnitude

of electrical conductance. In Fig. 2(a), the two resonances are located at t and $-t$, while with t and N increasing, the position of intiresonance has no changing.

Our results show that the thermopower S calculated by Eq. (30), it changes its sign whenV_g corresponds to one of the relevant resonances. The energy levels of quantum dots are tuned by gate potential, we set $E_n = -V_g$. When the energy levels of quantum dots is below μ (the leads chemical potential), the main carriers are holes (i.e. the charge and heat transport through the hole channels is predominant) and then $S$is positive. When the energy level is above μ, the main carriers are electrons (i.e. the charge and heat are carried by mainly electron channels) and thus $S$is negative [5]. So one can adjust the gate voltage or equivalently energy levels of quantum dots and obtain the optimized thermopower. By comparing Fig. 3 with the results in Fig. 2, we find that in the structure of T-shape-double-quantum dot, the antiresonance mechanism enhances the thermoelectric effect. And, with the increase of quantum dot numbers, the thermoelectric effect becomes more apparent. In Fig. 3, the thermo power increases when interdot interaction(t) increases at antiresonance. As we see the thermopower increases when the number of quantum dots increases at$t = 0.6\Gamma, \Gamma$, while at $t = 0.2\Gamma$, the thermopower decreases when the number of quantum dot increases.

In general, the electron thermal conductance calculated by Eq. (31), it is behaves the same as the electrical conductanceas shown in Fig. 4. But it is lower than electrical conductance, also appear added resonance at $V_g = 0$ when interdot tunneling $t = 0.2\Gamma$ for all values of N. After combine these three properties we get the thermoelectric efficiencyZT, which calculated by Eq. (32) (Fig. 5). The values of gate voltage at which the figure of merit vanishes corresponding to the same values at which S = 0. Figure of merit is considerably enhanced in the vicinity of the antiresonance position;outside this region ZT is significantly suppressed.In the structure of T-shape-double-quantum dot (Fig. 5(a)), we obtain the result that ZT <1 for all values of t. Therefore, when the number of quantum dots increases, the antiresonance mechanism can effectively cause the enhancement of the figure of merit at $t = 0.6\Gamma$ as shown in Figs. 5(b)-5(d).Except at N=10, ZT enhances at $= \Gamma$, see Fig. 5(e).

4. CONCLUSION

In summary, we have investigated thermoelectric properties, like electrical conductance, thermo power, electronic thermal conductance, and figure of merit in a system of serially coupled T-shape-double-quantum dot.

We have shownthat the antiresonance mechanism can significantly enhance thethermoelectric effects, especially for specific interdot interaction values. Figure of merit is considerably enhanced in the vicinity of the antiresonance position, outside this region ZT is significantly suppressed. The thermoelectric efficiency can be additionally enhanced by increasing the number of quantum dots. Thus, the thermoelectric efficiency can be controlled by adjusting gate voltage.

COMPETING INTERESTS

Authors have declared that no competing interests exist.

REFERENCES

1. AL-Badry LF. Theoretical study of the thermoelectric properties and performance efficiency for some nanostructured systems; 2014.
2. Trocha P, Barnaś Jz. Large enhancement of thermoelectric effects in a double quantum dot system due to interference and Coulomb correlation phenomena. Physical Review B. 2012;85:085408.
3. Gómez-Silva G, Avalos-Ovando O, MLLn. de Guevara, Orellana PA. Enhancement of thermoelectric efficiency and violation of the Wiedemann-Franz law due to Fano effect. Journal of Applied Physics. 2012;111:053704.
4. Kuo DMT, Chang YC. Effects of interdot hopping and Coulomb blockade on the thermoelectric properties of serially coupled quantum dots, Nanoscale research letters. 2012;7:1-6.
5. Niu ZP. Thermoelectric effects in a double-dot Aharonov-Bohm interferometer with Rashba spin-orbit interaction, The European Physical Journal B. 2011;82:153-158.
6. Kadel K, Kumari L, Li WZ, Huang JY, Provencio PP. Synthesis and thermoelectric properties of Bi2Se3 nanostructures. Nanoscale Res Lett. 2011;6:57.
7. Wang Y, Fan HJ. Improved thermoelectric properties of La_{1-x} Sr_x CoO_3 Nanowires. The Journal of Physical Chemistry C. 2010;114:13947-13953.
8. Soni A, Okram GS. Size-dependent thermopower in nanocrystalline nickel. Applied Physics Letters. 2009;95:013101-013101-013103.

9. Liu YS, Yang XF. Enhancement of thermoelectric efficiency in a double-quantum-dot molecular junction. Journal of Applied Physics. 2010;108:3710.
10. Zheng J, Zhu MJ, Chi F. Fano Effect on the Thermoelectric Efficiency in Parallel-Coupled Double Quantum Dots. Journal of Low Temperature Physics. 2012;166:208-217.
11. Hicks LD, Dresselhaus MS. Effect of quantum-well structures on the thermoelectric figure of merit. Physical Review B. 1993;47:12727.
12. Mahan GD, Sofo JO. The best thermoelectric. Proceedings of the National Academy of Sciences. 1996;93:7436-7439.
13. Zheng J, Chi F, Lu XD, Zhang KC. Thermoelectric effect in an Aharonov-Bohm ring with an embedded quantum dot. Nanoscale Research Letters. 2012;7:1-7.
14. Maslyuk VV, Achilles S, Mertig I. Spin-polarized transport and thermopower of organometallic nanocontacts. Solid State Communications. 2010;150:505-509.
15. Wierzbicki M, Swirkowicz R. Influence of interference effects on thermoelectric properties of double quantum dots. Physical Review B. 2011;84:075410.
16. Liu YS, Hong XK, Feng JF, Yang XF. Fano-Rashba effect in thermoelectricity of a double quantum dot molecular junction. Nanoscale Research Letters. 2011;6:1-10.
17. Han Y, Gong W, Wu H, Wei G. Decoupling and antiresonance in electronic transport through a quantum dot chain embodied in an Aharonov-Bohm interferometer, Physica B. Condensed Matter. 2009;404:2001-2007.
18. Solomon GC, Andrews DQ, Hansen T, Goldsmith RH, Wasielewski MR, Van Duyne RP, Ratner MA. Understanding quantum interference in coherent molecular conduction. The Journal of Chemical Physics. 2008;129:054701.
19. Moldoveanu V, Dinu IV, Tanatar B. Fano effect in a double T-shaped interferometer. The European Physical Journal B. 2009;67:231-238.
20. Calle AM, Pacheco M, Orellana PA. Fano effect and Andreev bound states in T-shape double quantum dots. Physics Letters A. 2013;377:1474-1478.
21. Ţifrea I, Crisan M, Grosu I. Evidence of quantum interference in transport properties of a triple quantum dot T-shape system. The European Physical Journal B. 2011;79:455-464.
22. Aldea A, Tolea M, Dinu IV. Peak-dip crossover of the differential conductance in mesoscopic systems with quantum impurities. In: Journal of Physics: Conference Series, IOP Publishing. 2009;022001.
23. Newns DM. Self-consistent model of hydrogen chemisorptions. Physical Review. 1969;178:1123.
24. Ballentine LE. Quantum mechanics: A modern development. World Scientific; 1998.
25. Kim TS, Hershfield S. Thermoelectric effects of an Aharonov-Bohm interferometer with an embedded quantum dot in the Kondo regim. Physical Review B. 2003;67:165313.
26. Sulston KW, Amos AT, Davison SG. Comparative study of approximate theoretical treatments of surface-ion neutralization. Surface Science. 1988;197:555-566.
27. Newns DM, Makoshi K, Brako R, vaN Wu Nnik JNM. Charge transfer in inelastic ion and atom-surface collisions. Physica Scripta. 1983;5.